

1 Gravimetric water distribution assessment from geoelectrical methods (ERT and EMI) in municipal
2 solid waste landfill

3 **Gaël Dumont^{a,*}, Tamara Pilawski^{ad}, Phidias Dzaomuh-Lenieregue^b, Serge Hiligsmann^b, Frank
4 Delvigne^b, Philippe Thonart^b, Tanguy Robert^{a1}, Frédéric Nguyen^a, Thomas Hermans^{ac2}**

5 ^aApplied Geophysics, GEO³ - ArGEnCo, Universtity of Liege, Quartier Polytech 1, Allée de la
6 Découverte 9, 4000 Liège, Belgium

7 ^bIndustrial Biochemistry and Microbiology, Universtity of Liege, Quartier Vallée 1, Chemin de la
8 vallée 2, 4000 Liège, Belgium

9 ^cPostdoctoral researcher at the F.R.S.-FNRS

10 ^dFRIA Grant Holder of the F.R.S.-FNRS

11 gumont@ulg.ac.be ; tamara.pilawski@ulg.ac.be ; t.robert@aquale.com ; P.Dzaomuh@ulg.ac.be ;

12 F.Delvigne@ulg.ac.be ; s.hiligsmann@ulg.ac.be ; p.thonart@ulg.ac.be ; F.Nguyen@ulg.ac.be ;

13 thomas.hermans@ulg.ac.be

14 **Corresponding author**

15 Dumont Gaël

16

17

18

19

¹ Now working at Aquale S.P.R.L., Ecofox Développement, Rue Ernest Montellier 22, 5380 Noville-les-Bois, Belgique

² Now at Stanford University, Department of Geological Sciences, 450 Serra Mall Bldg. 320 Rm.118 Stanford, CA 94305-2115, USA

20

21 **ABSTRACT**

22 The gravimetric water content of the waste material is a key parameter in waste biodegradation.
23 Previous studies suggest a correlation between changes in water content and modification of
24 electrical resistivity. This study, based on field work in Mont-Saint-Guibert landfill (Belgium), aimed,
25 on one hand, at characterizing the relationship between gravimetric water content and electrical
26 resistivity and on the other hand, at assessing geoelectrical methods as tools to characterize the
27 gravimetric water distribution in a landfill. Using excavated waste samples obtained after drilling, we
28 investigated the influences of the temperature, the liquid phase conductivity, the compaction and
29 the water content on the electrical resistivity. Our results demonstrate that Archie's law and
30 Campbell's law accurately describe these relationships in municipal solid waste (MSW). Next, we
31 conducted a geophysical survey *in situ* using two techniques: borehole electromagnetics (EM) and
32 electrical resistivity tomography (ERT). First, in order to validate the use of EM, EM values obtained *in*
33 *situ* were compared to electrical resistivity of excavated waste samples from corresponding depths.
34 The petrophysical laws were used to account for the change of environmental parameters
35 (temperature and compaction). A rather good correlation was obtained between direct
36 measurement on waste samples and borehole electromagnetic data. Second, ERT and EM were used
37 to acquire a spatial distribution of the electrical resistivity. Then, using the petrophysical laws, this
38 information was used to estimate the water content distribution. In summary, our results
39 demonstrate that geoelectrical methods represent a pertinent approach to characterize spatial
40 distribution of water content in municipal landfills when properly interpreted using ground truth
41 data. These methods might therefore prove to be valuable tools in waste biodegradation
42 optimization projects.

43 **KEYWORDS**

44 Electrical resistivity tomography; moisture content; leachate; municipal solid waste; bioreactor
45 landfill; borehole electromagnetic

46 **1. Introduction**

47 In Wallonia (Belgium), about 2500 landfills are present. Dozens of them are recognized as polluted
48 and hundreds of them potentially polluted (SPAQuE, 2003). Although there is no accurate landfill
49 counting in all the European countries, it has been estimates that 960000 landfills exists on the entire
50 continent (27 of the 39 countries collaborating with the European Environmental Agency (van
51 Liedekerke et al., 2014)). These numerous waste disposal sites represents a threat for the
52 environment and public health (air and groundwater pollution), covers valuable lands and brings high
53 exploitation and long duration post-exploitation cost.

54 Among the possible ways to deal with the waste issue, the concept of landfilling bioreactors has risen
55 in the last several years. These are new landfills designed and equipped to enable the monitoring and
56 manipulation of the humidity and oxygen content in the waste mass. In a landfill bioreactor, the
57 biodegradation of the organic waste is accelerated, which increases the production of landfill gas and
58 shortens the exploitation time. Moreover, biodegradation is more complete, which decreases
59 potential long-term pollution risks and therefore costs of post-exploitation monitoring. Finally, the
60 constant recirculation of leachate (which accumulates in the lower part of the landfill and is
61 reinjected in the upper part) reduces the costs of leachate treatment and evacuation (Audebert,
62 2015; Reinhart and Townsend, 1997).

63 An alternative approach is to equip existing municipal landfills in order to monitor the bioreactor-like
64 activities of the landfills. In Belgium, the MINERVE project, aims at transforming existing Belgian
65 municipal landfills into bioreactors so as to optimize the landfill biogas production. An additional
66 objective of the project is to study the landfill mining opportunity of the studied site

67 Water content is a limiting factor regarding the two objectives. Firstly, the bioreactor-like function of
68 a landfill highly depends on the waste water content, which affects both the completeness and the

69 kinetics of organic waste biodegradation (Benbelkacem et al., 2010; Šan and Onay, 2001). Secondly,
70 the humidity of the material influences the profitability of landfill mining operations. Indeed, the
71 moisture content affects the material separation efficiency (Ford et al., 2013). Any form of material
72 and energy recovery requires mechanical treatment (such as shredding, trommel screen or metal
73 extraction), the efficiency of which is limited by the water content, and may therefore also require an
74 expensive drying process (Fisher, 2013).

75 In this context, the moisture content of MSW landfills needs to be determined. Drilling followed by
76 waste sample analysis or punctual probes are the most direct ways to measure water content.
77 However, these techniques have proven itself very expensive and only provides punctual information
78 lacking spatial representativeness (Grellier et al., 2006a). Therefore, the interest in indirect
79 geophysical method development to determine water content has grown in the past few years
80 (Imhoff et al., 2007) and has been extensively studied in landfill bioreactors. Among the possible
81 geophysical ways to indirectly assess the moisture content of the waste mass, measuring the
82 electrical resistivity properties of waste has raised as a promising strategy (Grellier, 2005; Grellier et
83 al., 2007, 2006b; Guérin et al., 2004; Imhoff et al., 2007). A possible technique to achieve this is
84 Electrical resistivity tomography (ERT) which provides large scale distribution values of the electrical
85 resistivity of the waste material (Bernstone et al., 2000; Chambers et al., 2006, 2004). Most of the
86 time, time-lapse ERT is used to monitor changes in electrical resistivity linked to leachate content
87 variation during recirculation events or infiltration during rainfall events (Audebert et al., 2014;
88 Clément et al., 2011b, 2010; Grellier et al., 2008, 2006a; Guérin et al., 2004; Morris et al., 2003).
89 However, geophysical methods are not often used to directly measure water content (Grellier et al.,
90 2007).

91 In our study, we aimed at validating the electrical resistivity measurements as an indicator of water
92 content. Using direct measurements on excavated waste samples, we tried to understand the
93 influence of environmental factors such as temperature, compaction, leachate electrical conductivity

94 (resistivity) and leachate content parameters on electrical resistivity in order to establish a method to
95 correlate the electrical resistivity property of the waste with the moisture content. Once a direct
96 correlation between the electrical resistivity and the water content was established, we tested two
97 electrical geophysical methods to obtain spatially distributed information: the well-established
98 electrical resistivity tomography and, for the first time, borehole electromagnetics. These geophysical
99 techniques both appear as a reliable indirect and cost-effective means to determine the waste water
100 content.

101

102 **2. Site description and field testing**

103 All field tests are performed on one of the largest engineered landfill of Belgium, located in a former
104 sand quarry in Mont-Saint-Guibert (Figure 1). The 26 ha wide and up to 60 m deep (5,3 million m³ of
105 waste) site is under activity since 1958. Around 3 million tons of waste were landfilled prior to the
106 installation of a bottom high density polyethylene (HDPE) liner in the early 90s. Thereafter, the class
107 2 technical landfill exploitation license was renewed and 8 million tons were disposed. These are
108 composed of municipal solid waste, non-hazardous and non-toxic industrial waste and bulky waste
109 were disposed, as well as inert waste and clinker, mainly used for cover layers and dam and road
110 stability. The site infrastructure includes a bottom leachate collection system and 200 vertical gas
111 extraction wells. During the past 25 years, more than 1 billion m³ of landfill gas have been produced.
112 The waste is compacted with landfill compactors to conserve free space and maximize the landfill
113 lifespan.

114 In August 2012, a 32 m long borehole was drilled and equipped with HDPE pipes perforated for the
115 last 12 m. Temperature profiles (distributed temperature sensing method – DTS) and electrical
116 conductivity (borehole EM) were measured inside the boreholes. At the borehole location, the
117 landfill is 55m deep. A first disposal period occurred between 1995 and 2000, when a former ground
118 level was established (still partially in place 10 m below the current ground level). Then, an additional

119 10 m thick layer of waste was disposed in order to create the final topographic profile of the landfill
120 cell.

121 In May 2015, an electrical resistivity tomography perpendicular to the landfill ridge was performed
122 on the test site. The southern extremity of the profile is located on more recent waste (late 2009).
123 This is the less known part of the landfill with no boreholes, no leachate sample and no direct
124 measurement of the water table. The middle of the profile is the landfill ridge, characterized by flat
125 topography favoring water infiltration. The slope increases and reaches up to 15% in the northern
126 part.

127

128 **3. Material and methods**

129 The Electrical resistivity is a suitable physical parameter to study the water content of a landfill
130 (Guérin et al., 2004; Meju, 2006). The bulk resistivity varies with the water content, the composition,
131 the temperature and the compression state of the waste (e.g. Moreau et al., 2010). For the short-
132 term (a recirculation experiment for instance), changes in temperature and water content are the
133 most important effects. For the long-term (several months to several years), changes in the pore
134 water conductivity (resistivity) with maturation and aging of the landfill, as well as the waste
135 settlement, strongly influence the bulk resistivity.

136 **3.1. The electrical resistivity**

137 The electrical resistivity is expected to vary inversely with the moisture content. As electrical current
138 is mainly transported by the liquid phase inside the pores, waste with low moisture content has a
139 high electrical resistivity. The Archie's law (Archie, 1942; Wyllie and Gregory, 1953) describe the
140 evolution of the bulk resistivity with the fluid resistivity, the porosity, the saturation and some
141 coefficients related to the matrix structure. Grellier (2005) and Grellier et al. (2007) proposed a
142 simplified equation for the study of MSW. The volumetric water content replaces the porosity and
143 the saturation which are difficult to measure on waste sample:

144
$$\rho_b = \rho_w a \theta^{-m} = \sigma_w^{-1} a \theta^{-m} \quad (1)$$

145 Where ρ_b is bulk resistivity; ρ_w is resistivity of the pore fluid; a is the cementation constant; m is an
146 empiric constant and θ is the volumetric water content of the sample.

147 The influence of temperature on the electrical conductivity can be represented by a linear law based
148 on viscosity theory (Campbell et al., 1948). Generally, a 2% increase of conductivity with every
149 additional degree of temperature is observed. This theory has been validated experimentally for
150 MSW (Grellier, 2005; Grellier et al., 2006b).

151
$$\sigma = \sigma_{T_{ref}} \cdot \left(1 + c \cdot (T - T_{ref}) \right) \text{ where } c \simeq 2\%/^{\circ}C \text{ when } T_{ref} = 25^{\circ}C \quad (2)$$

152 Clément et al. (2011a) investigated the contribution of temperature, moisture content and dry
153 density feature to the bulk resistivity of waste. A ten coefficient equation is proposed and the most
154 significant parameters identified by statistical analysis. The moisture content and temperature
155 dominates the signal variation. While assessing the moisture content from the electrical resistivity
156 information, temperature variation cannot be neglected, while dry density variations are less
157 influent.

158 **3.2. Electric and electromagnetic geophysical methods**

159 Electrical and electromagnetic geophysical methods are suitable to characterize waste
160 deposits because of their sensitivity to electrical resistivity (Bernstone et al., 2000; Grellier et al.,
161 2007; Guérin et al., 2004).

162 The electrical resistivity tomography (ERT) method is widely described in many references (e.g.
163 Dahlin, 2001). An electrical current (I , in Ampere) is injected in the medium with a pair of stainless
164 steel electrodes and the resulting potential difference (ΔV , in Volt) is measured between two other
165 electrodes. This can be done at the laboratory scale (test cells) and at the field scale (ERT). For field
166 surveys, the greater the electrode spacing is, the larger and the deeper the investigated volume.
167 Hundreds or thousands of data are collected with various distances between current and potential

168 electrodes and then inverted with an iterative process to produce a 2D/3D representation of the
169 subsurface electrical resistivity that explains the measured data.

170 The ERT profile presented in this study is 410 m long (83 electrodes and 5 m electrode spacing). Its
171 extension is limited by road infrastructure around the landfill and the existence of a HDPE
172 membrane. Indeed, quadrupoles with electrodes both inside and outside the landfill are not
173 considered as the current flow would be prevented by the resistive membrane. Pinholes in the
174 geomembrane could even act as secondary electrodes, making the current flow pattern
175 unconventional (De Carlo et al., 2013; Tsourlos et al., 2014). The resistivity data were acquired with a
176 multiple-gradient protocol (Dahlin and Zhou, 2006) to take advantage of the multichannel ability of
177 the ABEM terrameter LS (Figure 2).

178 The data were inverted with the inversion code CRTomo (Kemna, 2000). The surface topography and
179 the bottom HDPE membrane morphology are included in the inversion grid with homogeneous
180 Neumann conditions (no current flow in normal direction) because the ERT profile is located too close
181 to the landfill HDPE membrane (both bottom liner and lateral boundary). Indeed, (Audebert et al.,
182 2014) have shown that a minimum distance of $0.64 \cdot L$ from the landfill boundary and $0.58 \cdot L$ from the
183 landfill bottom membrane (L is the ERT line total length) is necessary to neglect boundary effects.

184 The inversion process is based on the minimization of an objective function of the form (Tikhonov
185 and Arsenin, 1977):

$$186 \quad \phi = \|W_d(d - f(m))\|^2 + \lambda \|W_m m + \alpha(m - m_0)\|^2 \quad (3)$$

187 where the terms on the right hand-side are the data misfit constraint and the reference model
188 constraint (Oldenburg and Li, 1994). In equation 3, W_d is the data weighting matrix, f is the non-
189 linear operator mapping the log resistivities of the model m to the log impedance data set d . W_m is
190 the roughness matrix, λ is the regularization parameter, m_0 is a reference model and α weights the
191 importance of the reference model. W_d contains the error level on the data estimated from

192 reciprocal measurements (LaBrecque et al., 1996). The latter correspond to a measurement with the
193 same electrode quadrupole while exchanging the current electrodes with the potential electrodes. It
194 allows us to estimate the error level related to, among other phenomena, poor contact resistance.
195 An absolute error of 0.0005Ω and a relative error of 1% (the envelope of the reciprocal error model)
196 is considered during the inversion process (Slater et al., 2000), which provides a conservative error
197 model. The optimization process ends when the error weighted Chi^2 of the data misfit reaches 1 (i.e.
198 the data set is fitted within its error level assessed with reciprocal measurements). The reference
199 model is weighted (α coefficient) according to the faithfulness of the model. A high weight is used for
200 the saturated zone (well-known zones) so that resistivity value stays close to the imposed reference
201 model. A low weight is used for the unsaturated zone (uncertain zones) so that the resistivity values
202 are free to diverge from the reference model. Doing so, the weight given to the reference model is
203 important in zone of low sensitivity for ERT. Caterina et al. (2014) have shown with several examples
204 that including such prior information in the inversion helps to recover realistic resistivity
205 distributions. Similar weighted reference model schemes were already developed by several authors
206 (Blaschek et al., 2008; Karaoulis et al., 2014; Kim et al., 2014; Kim and Tsourlos, 2009; Yi et al., 2003).
207 The λ coefficient is optimized at each iteration to minimize the data misfit. At the last iteration, it is
208 increased to fit exactly the assumed level of noise.

209 To assess the quality of the ERT image at depth, we used the error weighted cumulative sensitivity
210 matrix (Caterina et al., 2013; Kemna, 2000). Note that when prior information is used, a low
211 sensitivity does not necessarily mean that the model is not reliable; it means that the regularization
212 has more importance than the data in this part of the tomogram (Hermans et al., 2012).

213 The borehole electromagnetic method provides the bulk electrical conductivity surrounding a
214 borehole using the inductive electromagnetic technique. We used the EM39 from GEONICS. The
215 radius of investigation is about 1m and the measurement is not influenced by the HDPE casing or the
216 fluid properties inside the borehole (McNeill, 1986). The response integrates a vertical interval of

217 about 1m. The EM measurement is strongly disturbed by metallic object in a 3 m radius around the
218 well, resulting in sharp deflection of the signal and sometimes loss of records (Taylor et al., 1989). In
219 September 2012, an electromagnetic log was performed in the boreholes. The EM conductivity
220 values were recorded at a 0.2 m interval in the landfill. In the unsaturated zone, within some depth
221 interval, negative values and very low values (irrelevant in the context of a landfill) were excluded
222 from the data set. An average mobile filter of one meter is applied to the data before interpretation.
223 For paper clarity, all EM measurements are later presented in terms of electrical resistivity.

224 The basic principle of the distributed temperature sensing (DTS) on fiber optic for borehole fluid
225 logging is described by Hurtig et al. (1994). We used the AP-Sensing linear pro series which operates
226 with a minimum spatial resolution as low as 50 cm and 0.1°C temperature resolution (spatial,
227 temperature and time resolution are interdependent). The borehole temperature log was recorded
228 simultaneously to the EM log.

229 **3.3. Borehole drilling, waste sampling and laboratory measurements**

230 Waste samples studied at the laboratory originate from a single 32 m long borehole
231 performed in August 2012 by auger drilling inside a steel casing. The drill bit was lifted every 4 m in
232 order not to mix all waste samples. The waste material was freed from the auger with a shovel, laid
233 out on a plastic sheet and then subsampled. The structure of the waste was strongly altered by the
234 drilling and sampling process so that the density, the solid matrix structure and the volumetric water
235 content was not representative of *in situ* conditions. Waste temperature was measured during the
236 drilling process whenever possible. The borehole was equipped with HDPE tubing screened on the
237 last 12m. A sample of leachate from the 15 m deep saturated zone was analyzed for the electrical
238 conductivity (resistivity).

239 Waste samples (30 dm³) were gathered every 2 m for further analysis. The gravimetric water content
240 is measured on a 1 dm³ subsample by weighting the mass loss after drying process (5 days at 55 °C).
241 Electrical resistivity laboratory measurements are performed on cylindrical transparent plastic tanks.

242 The bases of the cylinder are copper current transmission plates. Potential electrodes are located on
243 one generatrix of the cylinder and divide the tank in three equivalent volumes. The bulk electrical
244 resistivity measurement is based on a four point electrodes system. The geometric factor of both
245 tanks is given analytically by the Pouillet law:

$$246 \quad R = \rho_v \frac{h}{S} \quad (4)$$

247 Where R is the resistance, ρ_v is the resistivity, S is the surface of the current transmission plates and
248 h is the thickness of waste between the potential electrodes (one third of the cell total length). The
249 relation has been checked experimentally with water of known resistivity. A large cell, 9 dm³ in
250 volume (0.17 m diameter over 0.396 m in length) was used for electrical resistivity measurement on
251 waste samples issued from the borehole. For practical reasons (the 9 dm³ cell do not enter our
252 laboratory oven), a 1.5 dm³ cell (0.08 m diameter over 0.3 m in length) was used for temperature and
253 compression (volumetric water content) experiments.

254 The bulk resistivity of 13 waste samples originated from one single borehole (Table 1) was measured
255 in 9 dm³ test cells. The waste sample was compacted manually. The wet density of the sample is
256 measured in order to convert volumetric water content into gravimetric water content (equation 7)
257 and for later compaction state correction (equation 10). Thereafter, the liquid phase conductivity
258 (resistivity) is measured on 100-200 ml leachate sample recovered by pressing the waste with a 15
259 tons press.

260 The influence of temperature (10-65°C) on the waste resistivity and the influence of the volumetric
261 leachate content (through the compaction experiment) on the waste resistivity were validated in 1.5
262 dm³ cells. The first experiment was conducted on 1 waste sample and 4 leachate samples (presenting
263 different electrical conductivities) with similar results. The second experiment needed 18 waste
264 samples characterized by different water content and compaction state. The driest one contained
265 28.9% water. No liquid phase could be recovered through manual compaction. The last one (53% of
266 water) represents the largest water content encountered in our waste samples. For each of these

267 three samples, 6 different compaction works were applied (no compaction, 2.5, 5, 10 cm of material
268 added between two manual compaction steps with different compaction pressures between 1 and
269 10 t/m²) generating 18 different conditions. The waste sample dry density ranged from 0.24 to 0.63.
270 Geophysicists usually quantify the water content with the volumetric coefficient (θ), defined as the
271 volume of water (V_w) over the total volume (V_{total}) ratio, as it appears directly in the Archie's law.
272 This parameter strongly depends on the sampling procedure.

$$273 \quad \theta = \frac{V_w}{V_{total}} \quad (5)$$

274 On the other hand, microbial availability (for methane production) and sorting ability (for material
275 valorization) of the waste depends on the gravimetric water content (w), defined as the weight of
276 water (M_w) over the total sample weight (M_{total}) ratio. This parameter is independent of the density
277 of the waste and can be measured on disturbed samples (providing there is no desaturation).

$$278 \quad w = \frac{M_w}{M_{total}} \quad (6)$$

279 The relation between these two humidity parameters is straightforward, but practically, the *in situ*
280 wet density (D_{wet}) of a waste dump is very difficult to measure. The water density (D_w) is taken
281 equal to 1).

282

$$283 \quad \frac{\theta}{w} = \frac{v_w}{M_w} * \frac{M_{total}}{v_{total}} = \frac{D_{wet}}{D_w} \approx D_{wet} \quad (7)$$

284

285 **4. Results**

286 All measurements performed for this study aim at assessing the gravimetric water content of the
287 waste material. In a first approach, direct measurements of water content and bulk electrical
288 resistivity were performed on samples in the laboratory. Then, the ability of geophysical methods

289 (borehole EM and ERT) to provide reliable *in situ* distribution of water content in the waste material
290 is investigated.

291 **4.1. Laboratory**

292 The composition of waste samples looks relatively similar over the entire borehole, except for the
293 upper 2 samples (where silt and waste are mixed) and the samples located at 9 m and 11m
294 composed of a waste, silt and wood mixture (Table 1).

295 The gravimetric water content and the bulk resistivity of the samples are given in Table 1. The upper
296 15 m are unsaturated and characterized by a 20-27% gravimetric water content (with two humid
297 levels at 5 and 11 m depth), whereas samples below 15m depth originates from the saturated zone
298 and contain up to 55% of water. The visual humidity observations are not solely influenced by the
299 gravimetric water content but also the volumetric water content, and therefore the waste density.
300 This is the reason why a dense sample with 26% water (sample 19m) seems wetter than a loose
301 sample with 27.5% water (sample 13 m).

302 The bulk resistivity measured on samples decreases as depth increases (Table 1). The waste density
303 in test cell varied from 0.5 to 1.2 in an erratic behavior. A special care was needed for the
304 measurement on 5, 15 and 25 m depth sample for which the water content was clearly above the
305 retention capacity of the waste. These were energetically homogenized before any subsampling
306 and measurements were performed shortly after to limit sample desaturation.

307 The leachate conductivity varies from 7500 $\mu\text{S}/\text{cm}$ ($1.33 \Omega\cdot\text{m}$), for the surface and perched water
308 table, to 36000 $\mu\text{S}/\text{cm}$ ($0.28 \Omega\cdot\text{m}$) in the saturated zone (Table 1) (Figure 7d). In the unsaturated
309 zone, the leachate conductivity increases with depth. This could be accounted for by the progressive
310 dissolution of salt by the leachate during infiltration (the longer the contact time, the greater the
311 possibility for dissolving waste materials). However, some horizons are characterized by lower
312 conductivities, probably linked to preferential meteoric water arrival and accumulation. Increased
313 infiltration through the landfill cover layer is suspected at positions 220 m, 260 m and 315 (on ERT

314 profile at figure 5) due to flat topography or the existence of dams impeding the runoff process. In
315 contrast to the unsaturated zone, the leachate conductivity is more stable in the saturated zone
316 (excepted for sample 19m) and close to the mean leachate conductivity measured in the well after
317 equipment (34000 $\mu\text{S}/\text{cm}$; 0.29 $\Omega\cdot\text{m}$) (Figure 7 d).

318 The influence of temperature on the conductivity of 4 leachates and 1 waste samples was
319 investigated by performing one heating and cooling cycle in a laboratory oven. The temperature
320 increased from 10°C to 65°C, and then decreased again to check the reversibility of the process. For
321 the tested range of temperatures, a linear law based on the viscosity theory (Campbell et al., 1948)
322 fits the experimental data with a 2.101% increase of conductivity per degree of temperature
323 (reference temperature at 20°C; $R^2 = 1$).

$$324 \quad \sigma = \sigma_{20^\circ\text{C}} \cdot (1 + c \cdot (T - 20^\circ\text{C})) \text{ where } c = 2.101\% / ^\circ\text{C} \quad (8)$$

325 Using this relation, the *in situ* bulk resistivity (at the *in situ* temperature state) can be calculated from
326 bulk resistivity measurements performed in the laboratory at 20°C.

327 Next, the variation of the waste bulk resistivity with the volumetric water content was investigated
328 using reconstituted waste samples. For that purpose, three waste samples with different gravimetric
329 water content were prepared by adding different quantities of leachate to a preliminary oven dried
330 homogenized waste material originating from the 6 boreholes presented in figure 1. The entire range
331 of gravimetric water content observed in our samples (Figure 3) is covered. Figure 3 presents the
332 electrical resistivity data as a function of the volumetric water content, computed from the
333 gravimetric water content and the sample weight.

334 The waste resistivity appeared dominated by the volumetric water content. Indeed, two samples
335 with identical volumetric water content but different compression states and gravimetric water
336 contents are characterized by an identical bulk resistivity (Figure 3). Although the dry solid density,
337 the porosity and the tortuosity change with the compression state, the relation between the

338 electrical resistivity and the volumetric water content is describe by a single function derived from
339 Archie's law (equation 1).

$$340 \quad \rho_b = \rho_w a \theta^{-m} = 0.42 * 1.53 * \theta^{-2.101} \quad (9)$$

341

342 Where $\rho_w = 0.42 \Omega \cdot m$ (or $\sigma_w = 24000 \mu S/cm$) is the electrical resistivity of the liquid phase measured
343 with a conductivity probe, while a and m constants of the power law optimize the R^2 (0.99).

344 Assuming that the gravimetric water content is unchanged by the compression process (the
345 compaction was stopped when saturation was reached), the volumetric water content is
346 proportional to the wet density of the sample (equation 7). Based on these observations, Archie's
347 law (equation 1) expressed for the *in situ* wet density condition, divided by the same law expressed
348 for the laboratory wet density condition, can be used to reproduce the bulk resistivity representative
349 of the *in situ* compaction state from the laboratory bulk resistivity result and the *in situ* and
350 laboratory wet density ratio (equation 10).

$$351 \quad \rho_{b \text{ in situ}} = \rho_{b \text{ lab}} * \left(\frac{\theta_{\text{in situ}}}{\theta_{\text{lab}}} \right)^{-m} = \rho_{b \text{ lab}} * \left(\frac{D_{\text{in situ}}}{D_{\text{lab}}} \right)^{-m} \quad (10)$$

352

353 **4.2. Uncorrected field results**

354 An ERT tomography was acquired in May 2015, 32 months after the borehole acquisition. No major
355 change for the depth of water level and leachate conductivity was seen from 2012 to 2015. The
356 topographical features and the cover layer remain the same, no recirculation process occurred in
357 that specific zone, so that the perched water table highlighted in borehole data in 2012 is expected
358 to remain today.

359 The depth of investigation of the surface ERT is limited to 15-20m. Due to the high electrical
360 conductivity of the leachate, the model sensitivity rapidly decreases in depth (Figure 4). Due to the

361 high electrical conductivity of the leachate, the model sensitivity rapidly decreases in depth (Figure
362 4). In low sensitivity regions, a change of the model resistivity will have little or no influence on the
363 simulated data. This is typically found at greater depths. In those regions, the model resistivity are
364 not controlled by the measured data but by the reference or starting model used in the inversion
365 (Hermans et al., 2012). The latter corresponds to a homogeneous value equal to the waste resistivity
366 at depth (in the saturated zone) used to reproduce correct values below the water table.

367 On the inverted ERT profile (Figure 5) the saturated and unsaturated zones are clearly seen. Below 15
368 m, the saturated zone is characterized by a very low ($1-2 \Omega \cdot m$) and homogeneous resistivity. In
369 between, the unsaturated zone is characterized by a heterogeneous resistivity ($10-30 \Omega \cdot m$) that
370 could likely reflect local changes in the water content. Due to the weighted reference model
371 constraint, the depth to the saturated zone is consistent with the borehole data, even if the electrical
372 resistivity gradient is sharper in borehole data than with geophysical data acquired from the surface
373 (vertical resolution decreases with depth for surface ERT while it remains constant for borehole EM).
374 Some perched water tables are visible under the landfill ridge (position 220 m along ERT profile)
375 where a circulation drain is installed and at the exact position of our borehole (figure 1; figure 5).

376 Regarding the borehole EM data (Figure 6b), the saturated zone is 15 m deep (confirmed by
377 water table measurement) and is characterized by homogeneous resistivity of about $1 \Omega \cdot m$. The
378 unsaturated zone is more heterogeneous. A more sandy-silty layer is found at a 10m depth and
379 corresponds to a former impervious cover layer dating back from 2002. Above this layer, a less
380 resistive layer is visible at 5 m depth. In two vertical intervals (around 3 m and 7 m depth), a lot of
381 EM39 data had to be discarded, probably due to higher metal content in the waste material.

382 Three individual temperature measurement were performed in the well. During the drilling
383 process, the temperature was recorded by ourselves with a min/max thermometer. Data are
384 available at depth 3, 7, 19, 23, 27 and 31. These are in good accordance with DTS data measured
385 after borehole equipment but are missing around the unsaturated / saturated zones interface. The

386 temperature was also recorded by the drillers every time the drilling head was removed for waste
387 sampling. Measurements are always lower than DTS measures and are very heterogeneous. Finally,
388 DTS measurements are performed after the borehole equipment. DTS-measured temperature
389 changes inside the borehole are very smooth (Figure 6a). The saturated zone is nearly homogeneous
390 with temperature change between 57 and 61°C. The humid zone (10-15 m deep) is also characterized
391 by high temperature. The temperature gradient between the outside (25°C) and the 12 m deep
392 temperature (59°C) is nearly constant. In comparison with temperatures measured by the drillers
393 during the drilling process, temperature measurements in the borehole appear higher but also
394 smoother. This suggests that measurements taken during the drilling process are less reliable,
395 potentially because temperature probes are not placed in correct conditions, or because the probe
396 does not have enough time to reach an equilibrium. However, this also clearly shows that after
397 borehole equipment, the liquid and gas inside the casing undergo mixing and the temperature
398 heterogeneities will not be depicted by DTS measurement inside the well tubing.

399 **4.3. Interpretation**

400 Gravimetric water content increases while electrical resistivity (measured by ERT and by EM39)
401 decreases with depth. However, the laboratory results cannot be directly compared to field data.
402 First, the laboratory measurements were conducted at a room temperature of 20 °C while the *in situ*
403 temperatures vary from 25 to 65°C. Second, the waste density in test cell somehow varied from 0.5
404 to 1.2 kg/dm³. In order to compare data from different techniques collected *in situ* and in the
405 laboratory, the data need to be corrected for temperature and compression state (equations 8 and
406 10). A first strategy would be to bring laboratory measurements to *in situ* environmental conditions.
407 This way, laboratory data could validate EM39 and ERT data. Another strategy would be to correct
408 EM39 log and ERT profiles in order to remove the effect of temperature and density and thus infer
409 respectively the gravimetric water content profile and section (Grellier et al., 2007).

410 **4.3.1. Correction of laboratory results to reflect *in situ* conditions**

411 In the laboratory, resistivity measurements were performed at a constant temperature of
412 20°C (used for the reference temperature of equation 8). A 2.101% conductivity increase with every
413 degree of temperature is considered (equation 8). The temperature correction is based on the DTS
414 measurements performed in the borehole. The correction to apply is small close to the surface (air
415 temperature close to 20°C) but is significant at depth (nearly 50% conductivity increase – 33%
416 resistivity decrease – in the saturated zone; Figure 6c).

417 Regarding the compaction correction (equation 10), an *in situ* density of 0.9 at surface and 1.3-1.5 in
418 the saturated zone (with a gradient density in between) is retained (Figure 6a). This density profile is
419 based on “undisturbed waste sample” gathered at the same place in 2002 by the “bucket augering”
420 technique (smoothed by average mean). This range of density corresponds to normal to high
421 compaction rate (Zekkos et al., 2005). At low depth, the *in situ* density is smaller and easily
422 reproduced in the laboratory. In the saturated zone, densities are higher but the compression state is
423 also accurately reproduced in the laboratory. Reasons for this (e.g. preconsolidation strength, water
424 content, change of elasticity or particles size with aging of the waste) has not been investigated in
425 this study. The correction is predominant at intermediate depth (Figure 6c) where *in situ* densities
426 are non-satisfactorily reproducible in test cells.

427 While only a rough resistivity decrease with depth is observed on raw data (see section 4.1), a much
428 refined interpretation can be done from corrected data. Once the temperature (equation 8) and
429 compression (equation 10) correction applied, EM39 data correlate well with laboratory data (Figure
430 6b). In depth between 10 and 12 meters, the fit is not reliable. This issue might be explained by a
431 potential contamination of the waste sample during the drillings, which would originate in the
432 change in the casing diameter before the excavation of this particular sample. This hypothesis is
433 supported by the fact that both laboratory measurements (of water content and resistivity) are
434 correlated and differ from the *in situ* data. In order to compute the coefficient of determination,
435 laboratory measurement is compared to the more similar EM39 resistivity value in a small vertical

436 range (+- 20 cm) around sample position. Sample 11 m is probably contaminated and is discarded
437 from the data set. Doing so, the R^2 value is 0.85. Sample 9 m, located to a sharp vertical contrast of
438 resistivity (EM39 data) largely contributes to the R^2 deterioration. The uncertainty on the vertical
439 position of the sample 9 m could explain this observation. Indeed, the electrical resistivity value of
440 the sample 9 m is similar to the resistivity value of EM39 at 9.6 m depth. When sample 9 m is
441 discarded from the data set, the R^2 value reaches 1.

442 **4.3.2. Correction of *in situ* results to match laboratory conditions**

443 The gravimetric water content of the waste mass was computed from the electrical resistivity
444 *in situ* data. First, the coefficients deduced for the Archie's law and Campbell law (equation 8, 9 and
445 10) were used to compute the volumetric water content. Thereafter, the volumetric water content
446 was divided by the waste density to deduce the gravimetric water content (equation7). The same
447 process was applied to transform laboratory electrical resistivity data. The density taken into account
448 is the waste density inside the test cell.

449 For the leachate conductivity vertical profile, three different options were tested (Figure 7 a,b,c). The
450 first correction was applied with the real leachate conductivities measured on the liquid phase of the
451 sample (Table 1). This correction generated an optimal match between *in situ* and laboratory data
452 that validates the petrophysical laws described above. However, this correction is only valid locally,
453 for the EM39 data acquired in the same borehole (Figure 7a). Very humid level at 5, 11 and 15 m
454 depth are depicted in both data sets. The sample at 5 m is very humid but still relatively resistive
455 because the liquid phase of the sample is less conductive (more resistive) than the leachate. If we do
456 not consider this information, we could interpret the 5m depth layer as humid while it is saturated.
457 Laboratory analyses of the sample at 11m differ from *in situ* measurements. In this case, sample
458 contamination is suspected, more credits is given to EM39 data. Using real leachate conductivity (the
459 best correction we can reach so far), there is a strong correlation between measured water content
460 and computed water content from different methods (Figure 7a). The coefficient of determination

461 between direct and indirect water content measurement in the laboratory is rather high. The quality
462 of this fit is independent of the field temperature and density condition. However, the accuracy of
463 the liquid phase conductivity measurement and the gravimetric direct measurement
464 representativeness (very small samples were dried out) could explain the correlation factor ($R^2 =$
465 0.79; table 2).

466 Practically, once the petrophysical laws deduced for the site, our objective is to avoid the waste
467 sampling and subsequent laboratory analyses. Supposing we only have geophysical data and do not
468 have access to the liquid phase conductivity in the unsaturated zone, the average leachate
469 conductivity of 34000 $\mu\text{S}/\text{cm}$ measured in the borehole could be used for the correction (Figure 7b).
470 Provided that the leachate conductivity can be measured in several boreholes, the method can be
471 used to correct 2D/3D ERT tomographies. In our case, leachate conductivity varies between 30000
472 and 34000 $\mu\text{S}/\text{cm}$ in the different boreholes. Using a constant leachate conductivity value for the
473 correction provides us with an excellent fit in the saturated zone because the leachate conductivity
474 variations are small. In the unsaturated zone, the leachate conductivity is overestimated and
475 therefore, the computed water content is underestimated. For example, the liquid phase of the 5m-
476 sample is 8000 $\mu\text{S}/\text{cm}$, which is 4 times lower than the leachate conductivity measured in the well. As
477 a consequence, the computed water content is half the real humidity value ($2=4^{1/m}$). This layer
478 appears as dry (<30% humidity) while it is saturated above retention capacity and landfill mining
479 process and waste separation could be unexpectedly problematic in that zone. The coefficient of
480 determination for the entire data set is 0.54 (Table 2).

481 In a third intermediate solution, a conductivity gradient between the surface and the saturated zone
482 and a homogeneous liquid phase in the saturated zone is considered (Figure 7c). This hypothesis is
483 pertinently supported by our liquid phase conductivity measurements (Table 1). With the last
484 solution, the sample 5m is recognized as highly saturated. However, the sample 11m is not. The
485 leachate conductivity gradient hypothesis is therefore a compromise, generating more reliable

486 humidity data than the constant leachate hypothesis and that can be used at other location than the
487 borehole. The coefficient of determination is higher than for the constant liquid phase conductivity
488 hypotheses ($R^2 = 0.67$; table 2). A clearer improvement is observed on the average gravimetric water
489 content of the unsaturated zone with 29, 25, 23 and 16 % for the direct measurement, the real liquid
490 phase conductivity, the gradient liquid phase conductivity and the constant liquid phase conductivity
491 respectively.

492 **4.4. Mapping gravimetric water content from geophysical data**

493 While studying leachate recirculation process or the landfill mining opportunity of an entire site,
494 there is a real interest in providing spatially distributed values for the gravimetric water content. The
495 electrical resistivity tomography is the best suited geophysical method to produce 2D/3D images of
496 the underground electrical resistivity (later converted into water content) (Clément et al., 2010;
497 Grellier, 2005; Grellier et al., 2007; Guérin et al., 2004; Imhoff et al., 2007).

498
499 Following the procedure described in section 2.3.2, the gravimetric water content was computed
500 from the ERT profile. For that purpose, the density, the temperature and the liquid phase
501 conductivity distribution on the entire 2D profile had to be known. In this study, the vertical logs
502 observed around the borehole are extrapolated to the entire field. The leachate conductivity in the
503 saturated zone was checked in 5 other boreholes (leachate conductivity ranges from 27000 to 34000
504 $\mu\text{S}/\text{cm}$) on the landfill. However, none of these boreholes is located on the south eastern part of the
505 ERT profile. The gravimetric water 2D distribution is illustrated in Figure 8. There is a clear distinction
506 between the saturated (30-35 % water) and the unsaturated zone (10-30% water). Under the landfill
507 ridge and the drilling zone, some humid pockets of waste are visible, probably resulting from water
508 infiltration through the capping. At 10 meter depth, a nearly continuum of dry waste is visible (except
509 under the landfill ridge). This layer reaches the surface after position 330m (towards the north-west).
510 The existence of this low humidity layer is confirmed at the drilling position by borehole EM and

511 laboratory data. We suspect a very low vertical permeability layer, with no clear evidence of it in the
512 drillings cuttings, between the perched water table (at 5 m depth) and rather dry deeper layers.

513 The electrical resistivity information extracted from the ERT profile at the borehole location was
514 compared to EM borehole data and laboratory corrected measurements (Figure 9a). ERT data
515 appears generally higher and smoother. The perched water table at 5 m depth is clearly visible but
516 the resistivity contrast with the other layers is reduced. The resistive layer at 10 m depth is correctly
517 retrieved but the extremely low resistivity layer at 15 m depth is not. In the saturated zone, as the
518 sensitivity decreases with depth, the resulting tomography is constrained by the reference model.

519 Below 20 m depth, the model matches the reference model ($1 \Omega\cdot\text{m}$). The gravimetric water content
520 extracted from the ERT profile at the borehole location with the gradient liquid phase conductivity
521 hypothesis is illustrated in Figure 9b. The humid level at 5 m depth is clearly visible but the value is
522 much lower. This is not unexpected since the real leachate conductivity (quite low) is not taken into
523 account in the correction process. At 10 m depth, a dry level is present. The ERT data are in
524 accordance with EM39 values. The waste sample analyses differs but are supposed to be
525 contaminated at that specific depth. At that depth, a thin low resistivity horizon would probably not
526 have been visible in the ERT profile due to the smoothness constraint used for the inversion
527 stabilization. For the same reason, the extremely low resistivity horizon at 15 m depth visible on
528 EM39 data and laboratory measurements is not visible on the ERT data.

529 **5. Discussion**

530 The results of this study show that the water content of municipal solid waste can be estimated from
531 its bulk resistivity, provided that some parameters, namely the temperature, the density and the
532 liquid phase conductivity, are known or estimated. Petrophysical laws describing the influence of
533 these parameters on the bulk resistivity of a waste sample were determined through laboratory
534 experimentation and were successfully used to correct resistivity measurement over the entire
535 length of the borehole. These results are also supported by previous reports showing that electrical

536 resistivity tomography can be successfully converted into gravimetric water content distribution in a
537 less complex environment (Grellier et al., 2007, 2006b).

538 The rather good correlation between direct (weight loss through drying process) and indirect methods
539 (resistivity measurement in laboratory, ERT and borehole electromagnetics *in situ*) to measure the
540 gravimetric water content suggests that empirical models are sufficient to describe the resistivity
541 variation in the range of temperature and density encountered in a landfill. However the
542 petrophysical laws probably need to be recalibrated for other landfills or even different zones of the
543 same landfill.

544 An estimation of the temperature, density and leachate conductivity distribution in the entire landfill
545 is needed to convert resistivity in water content. While these parameters are measured with a high
546 precision in a laboratory, the *in situ* parameters are generally poorly described. In the literature, the
547 density and leachate conductivity is often considered as a constant (e.g., Grellier et al., 2007) as a
548 first approximation. This study shows that the distribution of these parameters is better described by
549 gradient in the unsaturated zone and constant in the saturated zone. This situation is a reasonable
550 assumption already made for temperature (measure in a borehole) and density (averaged data) and
551 can be used for both ERT and borehole EM data interpretation. However, the leachate conductivity
552 gradient is probably strongly site dependent and varies with the rainfall events on the area, the type
553 of cover layer (silt, clay, HDPE membrane) or the inclination of the ground level. While assessing the
554 gravimetric water content from geoelectrical methods, the limiting factor is the evaluation of the
555 waste resistivity, temperature and density profiles rather than the petrophysical law itself.

556 The metallic content of the waste material might be a limiting factor for the use of borehole
557 electromagnetics. In this study, the method was successfully used after removal of outliers
558 originating from high metallic content zones. The metal content in municipal solid waste all around
559 the world is estimated to 3, 2-3 and 6 % in lower, middle and upper income countries (Hoornweg and
560 Bhada-Tata, 2012). In the present case, the content is limited to 3.5% in weight, resulting from

561 efficient Belgian waste sorting policy. The method need further validation for high metallic content
562 landfills, whereas regarding global statistics, it should be reliable on most sites.

563 The quality of the ERT inversion in such a complex media is a real challenge. For this study, we had to
564 impose the water table depth in the prior model of the ERT inversion in order to produce plausible
565 resistivity values. If we impose an incorrect water table as prior information in the reference model
566 constraint, the inversion still converges but to impossible values. Likewise, if we do not guide the
567 inversion process by imposing the saturated zone electrical resistivity, the saturated zone is retrieved
568 with a resistivity value of 3-4 $\Omega\cdot\text{m}$ (instead of 1 $\Omega\cdot\text{m}$). While the structural interpretation is still
569 straightforward, conversion to water content through petrophysical laws would lead to low humidity
570 values (15-20 %) in the saturated zones. Ground truth data are mandatory to ensure the quality of
571 inversion results. Borehole EM data could also be used as prior information to further improve the
572 ERT inversion (e.g. Caterina et al., 2014).

573 With increasing projects of leachate recirculation process, there is an increasing demand for time-
574 lapse monitoring of water content inside a landfill. The observation of resistivity changes appears less
575 challenging than direct correlation between resistivity and water content. However, the
576 interpretation of monitoring data is difficult due to the multiple factors influencing the resistivity.
577 Waste maturation involves changes in leachate salinity, settlement (and therefore change in
578 saturation), and heat production trough microbial activity. Recirculation or infiltration or fresh
579 leachate / water process imply changes in leachate salinity, temperature and saturation.
580 Theoretically, borehole measurements could be repeated from time to time to provide time-lapse
581 high vertical resolution information. In practice, boreholes are rapidly sheared due to differential
582 settlement of the waste. In the specific study, the borehole integrity was no more ensured after a
583 few months.

584 **6. Conclusions**

585 A borehole has been drilled on a municipal landfill site of Belgium. Waste samples were collected
586 every 2 meters and analyzed for the gravimetric water content and the bulk electrical resistivity. We
587 validated the use of long-established petrophysical laws to describe the influence of the
588 temperature, the compaction and the volumetric water content on the waste resistivity of the waste
589 material. Empirical parameters for these laws were defined to allow the calculation of the
590 gravimetric water content from the bulk electrical resistivity, the temperature, the density and the
591 liquid phase electrical conductivity information.

592 With the electrical resistivity tomography (or ERT) and borehole electromagnetics (or EM), we have
593 shown that, on one hand, bulk electrical resistivity measured on waste sample (in the laboratory) and
594 in the borehole present an excellent correlation once the data are corrected for their temperature
595 and compaction environment. On the other hand, we have established that two geophysical
596 methods, ERT and borehole EM, can be used to estimate the moisture content over large areas,
597 provided that environmental parameters measured at one place are proved to be representatives of
598 the entire site or that this parameters are known at several location in the landfill.

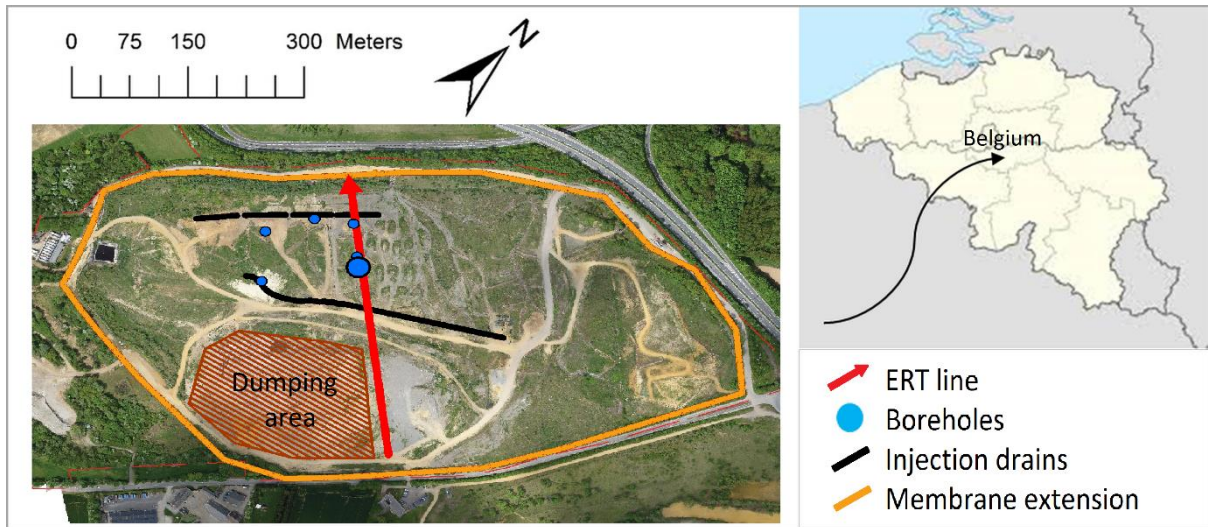
599 Given the importance of the water content of the waste material for the biodegradation of the
600 organic waste biodegradation process and in a later phase of the landfill exploitation, the feasibility
601 of landfill mining, the present methodology opens perspective for large scale site characterization.

602 **7. Acknowledgements**

603 The MINERVE project is a multidisciplinary research program financed by the Walloon Region (Plan
604 Marshall2.vert, pôle GreenWin; <http://greenwinminerve.com/>). We are grateful to SHANKS, the
605 leader of the research program for the access to the site and technical support; the Industrial
606 Biochemistry and Microbiology ULg units for the gravimetric water content measurement on waste
607 samples and the Centre Terre & Pierre (CTP) for metal content measurements.

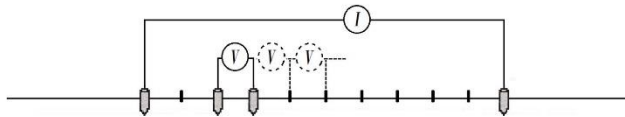
608

609 **Figure**



610

611 *Figure 1: Location of Mont-Saint-Guibert engineered landfill (Belgium). The geophysical survey layout is depicted as a red*
612 *arrow; boreholes location as blue dots (oversized for the borehole described in the present paper); Injection drains as black*
613 *lines and the HDPE membrane extension as orange contour.*



614

615 *Figure 2: The multiple-gradient electrode protocol electrode configuration*

616

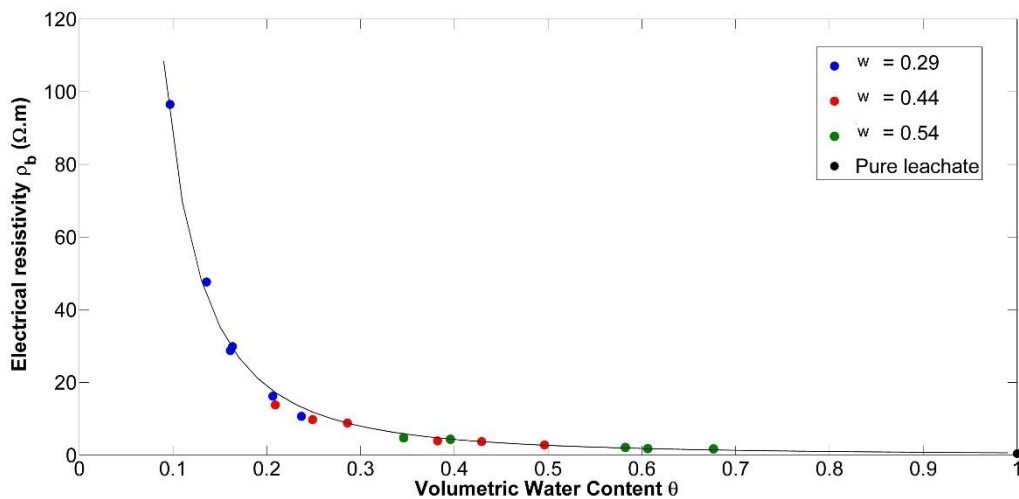
SAMPLE DEPTH (M)	LABORATORY RESULTS (20°C)			VISUAL OBSERVATION		LEACHATE CONDUCTIVITY (μS/CM)
	Grav. Water content	Bulk resistivity (Ω·m)	Sample density	Humidity	Composition	
1	0.245	86.03	0.87	dry	Silt + waste	7500
3	0.273	63.62	0.673	dry	Waste + silt	14750
5	0.477	10.13	0.99	> retention capacity	waste	8000
7	0.239	25.04	0.754	dry	waste	23000
9	0.214	82.59	0.617	dry	Silt + wood + waste	24300
11	0.471	28.14	0.557	humid	Silt + wood + waste	11760
13	0.275	31.63	0.736	dry	waste	17370
15	0.557	1.926	0.935	> retention capacity	waste	30850
17	0.368	13.69	0.641	Very humid	waste	31800
19	0.259	8.56	1.049	humid	waste	17200
21	<i>Lost sample</i>					
23	0.360	4.737	0.934	Very humid	waste	30800
25	0.375	1.898	1.047	> retention capacity	waste	32000
27	<i>Lost sample</i>					
29	0.341	1.813	1.173	Very humid	waste	36000
31	<i>Lost sample</i>					

617

618 *Table 1: observation and measures made in the laboratory on waste samples collected during drilling process. The*

619 *gravimetric water content is measured after drying a 1 dm³ waste sample, the bulk resistivity and the waste wet density are*

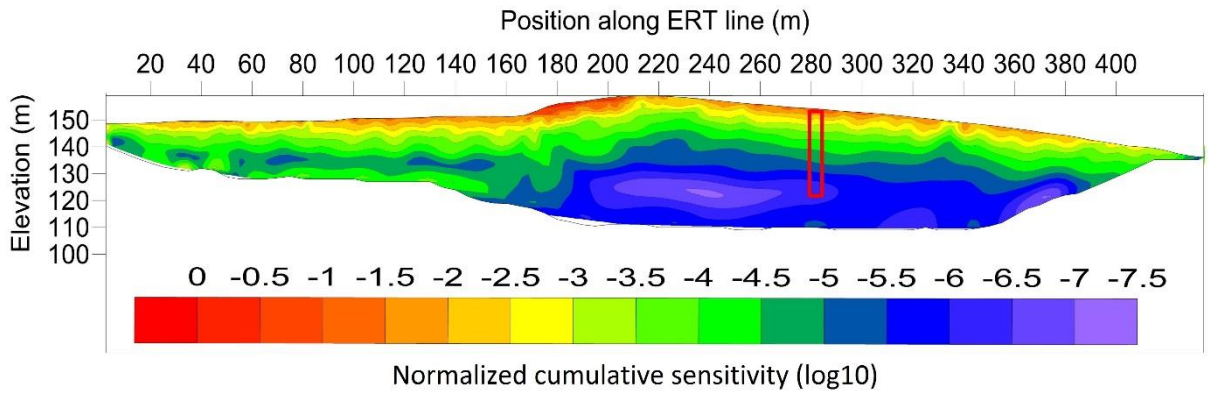
620 *measured on a 9 dm³ waste sample.*



621

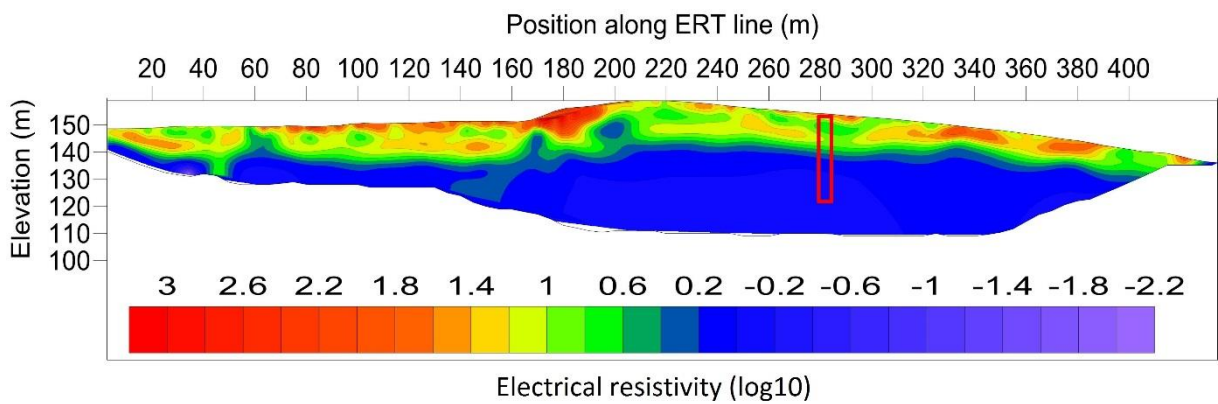
622 *Figure 3 : Bulk electrical resistivity of a waste sample as a function of the volumetric water content. 18 samples are tested (3*

623 *gravimetric water content * 6 compression states). The volumetric water content 100% stand for the pure leachate resistivity.*



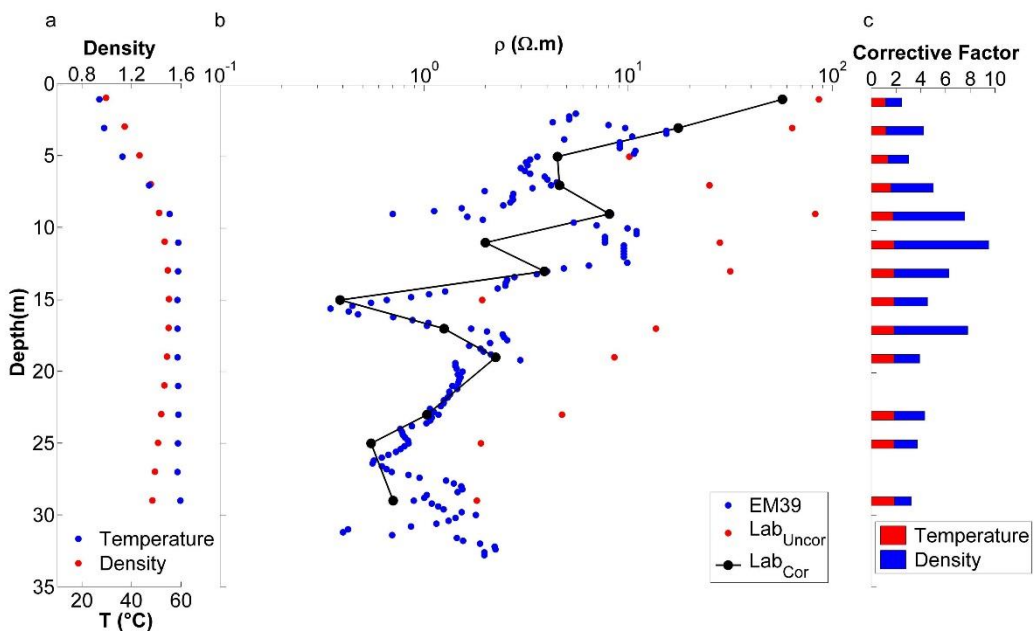
624

625 *Figure 4: cumulative sensitivity value (log10). The sensitivity value rapidly decrease with depth due to the high electrical*
 626 *conductivity of the leachate.*



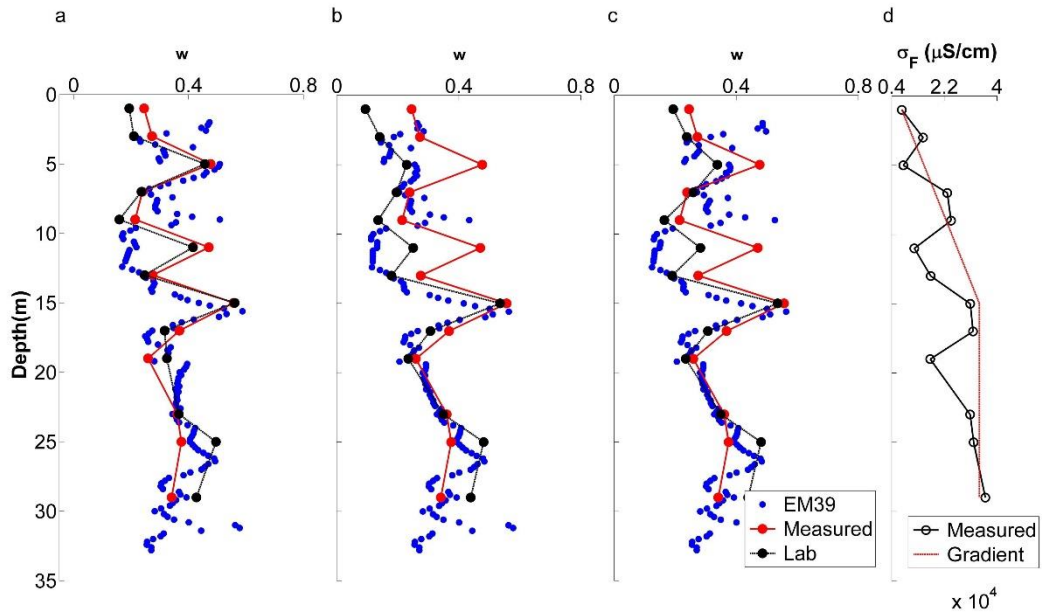
627

628 *Figure 5: Electrical resistivity tomography (log10 of electrical resistivity) crossing the landfill from the SE border to the NW*
 629 *border. The inversion process ended with an error weighted χ^2 equal to 1 (see section 3.2.) and a final regularization*
 630 *parameter (λ) equal to 0.7.*



631

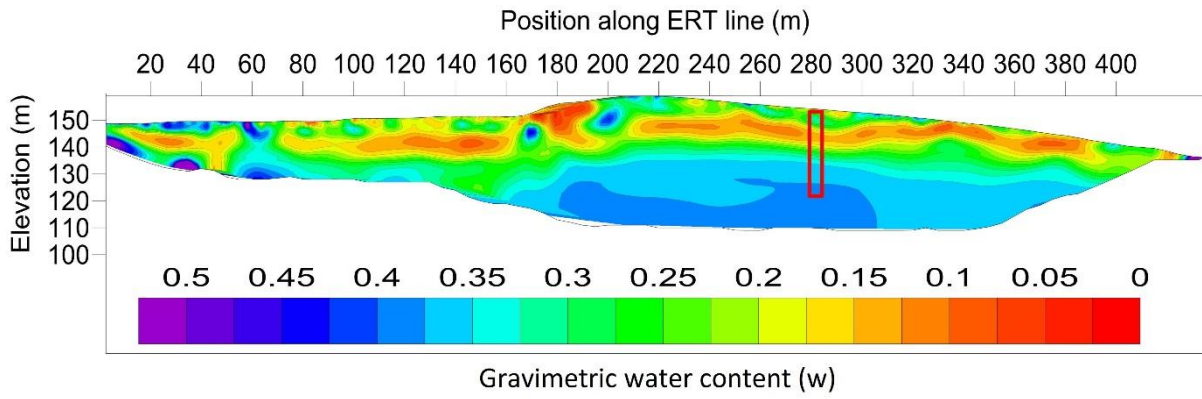
632 Figure 6: resistivity measurement in borehole K6 and measurement correction: a. in situ temperature and density profiles; b.
 633 electrical geophysical method (borehole EM) vs bulk resistivity measured on waste sample (uncorrected and corrected); c.
 634 relative importance of the temperature and the compaction correction.



635
 636 Figure 7: Waste gravimetric water content for three methods (direct measurement in the laboratory, from resistivity measures
 637 in laboratory and from borehole EM in situ) and three hypothesis for the liquid phase conductivity: a. measured liquid phase
 638 conductivity; b. constant liquid phase conductivity; c. liquid phase conductivity gradient in the unsaturated zone; d. measured
 639 liquid phase conductivity and gradient / constant liquid phase conductivity hypothesis

Coefficient of determination (R^2)	Hypothesis on the liquid phase conductivity		
	Real	Gradient	Constant
Indirect laboratory VS direct laboratory	0.79	0.67	0.54
EM39 VS direct laboratory	0.89	0.79	0.54

640
 641 Table 2: correlation between the gravimetric water content values computed with three different method: direct laboratory
 642 measurement (mass loss trough drying process), indirect laboratory measurements (bulk electrical resistivity measured on
 643 waste sample) and borehole EM (EM39).



644

645

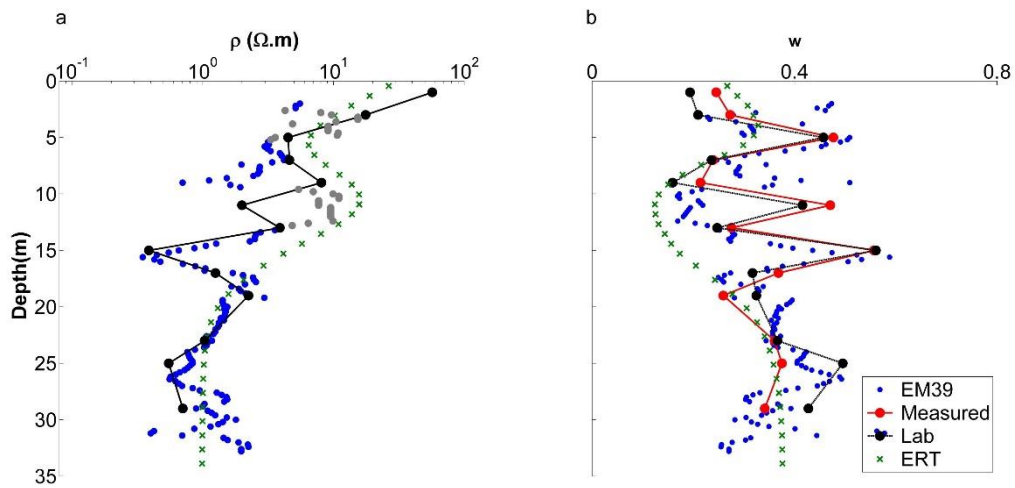
Figure 8: Gravimetric water content inside the landfill. Humidity value are calculated from the electrical resistivity

646

tomography and temperature / density condition measured in situ. For the liquid phase conductivity, the conductivity

647

gradient hypothesis is used in the unsaturated zone.



648

649

650

Figure 9 : a. electrical resistivity distribution around the borehole; b. gravimetric water distribution around the borehole

651

652

- 654 Archie, G.E., 1942. The electrical resistivity log as an aid in determining some reservoir
655 characteristics. *Trans. Am. Inst. Min. Metall. Pet. Eng.* 146, 54–67.
- 656 Audebert, M., 2015. Développement d'une méthode de contrainte des modèles hydrodynamiques
657 par une stratégie d'analyse des données géophysiques ERT : Application aux écoulements de
658 lixiviat dans les massifs de déchets. Université Grenoble Alpes, Grenoble, France.
- 659 Audebert, M., Clément, R., Grossin-Debattista, J., Günther, T., Touze-Foltz, N., Moreau, S., 2014.
660 Influence of the geomembrane on time-lapse ERT measurements for leachate injection
661 monitoring. *Waste Manag.* 34, 780–790. doi:10.1016/j.wasman.2014.01.011
- 662 Benbelkacem, H., Bayard, R., Abdelhay, A., Zhang, Y., Gourdon, R., 2010. Effect of leachate injection
663 modes on municipal solid waste degradation in anaerobic bioreactor. *Bioresour. Technol.*
664 101, 5206–5212. doi:10.1016/j.biortech.2010.02.049
- 665 Bernstone, C., Dahlin, T., Ohlsson, T., Hogland, H., 2000. DC-resistivity mapping of internal landfill
666 structures: two pre-excitation surveys. *Environ. Geol.* 39, 360–371.
667 doi:10.1007/s002540050015
- 668 Blaschek, R., Hördt, A., Kemna, A., 2008. A new sensitivity-controlled focusing regularization scheme
669 for the inversion of induced polarization data based on the minimum gradient support.
670 *Geophysics* 73, F45–F54. doi:10.1190/1.2824820
- 671 Campbell, R., Bower, C., Richards, L., 1948. Change of electrical conductivity with temperature and
672 the relation of osmotic pressure to electrical conductivity and ion concentration in soil
673 extracts. *Soil Sci. Soc. Am. Proc.* 13, 66–69.
- 674 Caterina, D., Beaujean, J., Robert, T., Nguyen, F., 2013. A comparison study of different image
675 appraisal tools for electrical resistivity tomography. *Surf. Geophys.* 11, 639–657.
676 doi:10.3997/1873-0604.2013022
- 677 Caterina, D., Hermans, T., Nguyen, F., 2014. Case studies of incorporation of prior information in
678 electrical resistivity tomography: comparison of different approaches. *Surf. Geophys.* 12,
679 451–465. doi:10.3997/1873-0604.2013070
- 680 Chambers, J.E., Meldrum, P., Kuras, O., Ogilvy, R.D., Hollands, J., 2004. Investigation of a former
681 quarry and landfill site using electrical resistivity tomography. Presented at the Near Surface
682 2004 - 10th European Meeting of Environmental and Engineering Geophysics, Utrecht, The
683 Netherlands.
- 684 Chambers, J., Kuras, O., Meldrum, P., Ogilvy, R., Hollands, J., 2006. Electrical resistivity tomography
685 applied to geologic, hydrogeologic, and engineering investigations at a former waste-disposal
686 site. *Geophysics* 71, 231–239. doi:10.1190/1.2360184
- 687 Clément, R., Descloitres, M., Günther, T., Oxarango, L., Morra, C., Laurent, J.-P., Gourc, J.-P., 2010.
688 Improvement of electrical resistivity tomography for leachate injection monitoring. *Waste*
689 *Manag.* 30, 452–464. doi:10.1016/j.wasman.2009.10.002
- 690 Clément, R., Moreau, S., Günther, T., 2011a. Estimating the Effect of Temperature, Density and
691 Water Content on Waste Electrical Resistivity. Presented at the Near Surface 2011 – 17 th
692 European Meeting of Environmental and Engineering Geophysics, Leicester, UK.
- 693 Clément, R., Oxarango, L., Descloitres, M., 2011b. Contribution of 3-D time-lapse ERT to the study of
694 leachate recirculation in a landfill. *Waste Manag.* 31, 457–467.
695 doi:10.1016/j.wasman.2010.09.005
- 696 Dahlin, T., 2001. The development of DC resistivity imaging techniques. *Comput. Geosci.* 27, 1019–
697 1029. doi:10.1016/S0098-3004(00)00160-6
- 698 Dahlin, T., Zhou, B., 2006. Multiple-gradient array measurements for multichannel 2D resistivity
699 imaging. *Surf. Geophys.* 4, 113–123. doi:10.3997/1873-0604.2005037
- 700 De Carlo, L., Perri, M.T., Caputo, M.C., Deiana, R., Vurro, M., Cassiani, G., 2013. Characterization of a
701 dismissed landfill via electrical resistivity tomography and mise-à-la-masse method. *J. Appl.*
702 *Geophys.* 98, 1–10. doi:10.1016/j.jappgeo.2013.07.010

703 Fisher, R., 2013. Landfill mining, Key Issue Paper. International Solid Waste Association, Cranfield
704 University, UK.

705 Ford, S., Warren, K., Lorton, C., Smithers, R., Read, A., Hudgins, M., 2013. Feasibility and Viability of
706 Landfill Mining and Reclamation in Scotland. Ricardo - AEA, for Zero Waste Scotland, UK.

707 Grellier, S., 2005. Suivi hydrologique des centres de stockage de déchet-bioréacteurs par mesures
708 géophysiques. Université Paris VI, Paris, France.

709 Grellier, S., Guérin, R., Robain, H., Bobachev, A., Vermeersch, F., Tabbagh, A., 2008. Monitoring of
710 leachate recirculation in a bioreactor landfill by 2-D electrical resistivity imaging. *J. Environ.*
711 *Eng. Geophys.* 13, 351–359.

712 Grellier, S., Reddy, K., Gangathulasi, J., Adib, R., Peters, A., 2006a. Electrical Resistivity Tomography
713 Imaging of Leachate Recirculation in Orchard Hills Landfill, in: *Proceedings of the SWANA*
714 *Conference*. Charlotte.

715 Grellier, S., Reddy, K., Gangathulasi, J., Adib, R., Peters, C., 2007. Correlation between Electrical
716 Resistivity and Moisture Content of Municipal Solid Waste in Bioreactor Landfill. *Geotech.*
717 *Spec. Publ.* 1–14.

718 Grellier, S., Robain, H., Bellier, G., Skhiri, N., 2006b. Influence of temperature on the electrical
719 conductivity of leachate from municipal solid waste. *J. Hazard. Mater.* 137, 612–617.
720 doi:10.1016/j.jhazmat.2006.02.049

721 Guérin, R., Munoz, M.L., Aran, C., Laperrelle, C., Hidra, M., Drouart, E., Grellier, S., 2004. Leachate
722 recirculation: moisture content assessment by means of a geophysical technique. *Waste*
723 *Manag.* 24, 785–794. doi:10.1016/j.wasman.2004.03.010

724 Hermans, T., Vandenbohede, A., Lebbe, L., Martin, R., Kemna, A., Beaujean, J., Nguyen, F., 2012.
725 Imaging artificial salt water infiltration using electrical resistivity tomography constrained by
726 geostatistical data. *J. Hydrol.* 438-439, 168–180. doi:10.1016/j.jhydrol.2012.03.021

727 Hoornweg, D., Bhada-Tata, P., 2012. What a waste: a global review of solid waste management.
728 World Bank, Washington DC.

729 Hurtig, E., Großwig, S., Jobmann, M., Kühn, K., Marschall, P., 1994. Fibre-optic temperature
730 measurements in shallow boreholes: experimental application for fluid logging. *Geothermics*
731 23, 355–364. doi:10.1016/0375-6505(94)90030-2

732 Imhoff, P., Reinhart, D., Englund, M., Guérin, R., Gawande, N., Han, B., Jonnalagadda, S., Townsend,
733 T., Yazdani, R., 2007. Review of state of the art methods for measuring water in landfills.
734 *Waste Manag.* 27, 729–745. doi:10.1016/j.wasman.2006.03.024

735 Karaoulis, M., Tsourlos, P., Kim, J.-H., Revill, A., 2014. 4D time-lapse ERT inversion: Introducing
736 combined time and space constraints. *Surf. Geophys.* 12, 25–34. doi:10.3997/1873-
737 0604.2013004

738 Kemna, A., 2000. Tomographic Inversion of Complex Resistivity-Theory and Application. Ruhr-
739 Universität, Bochum, Germany.

740 Kim, J.H., Tsourlos, P., 2009. ERT inversion with a priori information. Presented at the Near Surface
741 2009 - 15th European Meeting of Environmental and Engineering Geophysics, Dublin,
742 Irlande.

743 Kim, J.H., Tsourlos, P., Yi, M.-J., Karmis, P., 2014. Inversion of ERT data with a priori information using
744 variable weighting factors. *J. Appl. Geophys.* 105, 1–9. doi:10.1016/j.jappgeo.2014.03.003

745 LaBrecque, D.J., Miletto, M., Daily, W., Ramirez, A., Owen, E., 1996. The effects of noise on Occam's
746 inversion of resistivity tomography data. *Geophysics* 61, 538–548.

747 McNeill, J.D., 1986. Geonics EM39 Borehole Conductivity Meter: Theory of Operation (No. TN-20).
748 Geonics Ltd., Ontario, Canada.

749 Meju, M., 2006. Geoelectrical characterization of covered landfill sites: a process-oriented model and
750 Investigative approach, in: *Applied Hydrogeophysics*. Springer, pp. 319–339.

751 Moreau, S., Ripaud, F., Saidi, F., Bouyé, J.-M., 2010. Laboratory test to study waste moisture from
752 resistivity. *Proc. ICE - Waste Resour. Manag.* 164, 17–30. doi:10.1680/warm.900025

753 Morris, J.W., Vasuki, N., Baker, J., Pendleton, C., 2003. Findings from long-term monitoring studies
754 at MSW landfill facilities with leachate recirculation. *Waste Manag.* 23, 653–666.
755 doi:10.1016/S0956-053X(03)00098-9
756 Oldenburg, D.W., Li, Y., 1994. Subspace linear inverse method. *Inverse Probl.* 10, 915–935.
757 Reinhart, D.R., Townsend, T.G., 1997. *Landfill Bioreactor Design and Operation*. Lewis Publishers,
758 Boca Raton.
759 Šan, I., Onay, T.T., 2001. Impact of various leachate recirculation regimes on municipal solid waste
760 degradation. *J. Hazard. Mater.* 87, 259–271. doi:10.1016/S0304-3894(01)00290-4
761 Slater, L., Binley, A., Daily, W., Johnson, R., 2000. Cross-hole electrical imaging of a controlled saline
762 tracer injection. *J. Appl. Geophys.* 44, 85–102. doi:10.1016/S0926-9851(00)00002-1
763 SPAQuE, 2003. *Rapport annuel*. SPAQuE, Liège.
764 Taylor, K.C., Hess, J.W., Mazzela, A., 1989. Field Evaluation of a Slim-Hole Borehole Induction Tool.
765 *Ground Water Monit. Remediat.* 9, 100–104. doi:10.1111/j.1745-6592.1989.tb01125.x
766 Tikhonov, A.N., Arsenin, V.I., 1977. *Solutions of ill-posed problems*. Winston and Sons, Washington.
767 Tsourlos, P., Vargemesis, G.N., Fikos, I., Tsokas, G.N., 2014. DC geoelectrical methods applied to
768 landfill investigation: case studies from Greece. *First Break* 32, 81–89.
769 van Liedekerke, M., Prokop, G., Rabl-Berger, S., Kibblewhite, M., Louwagie, G., 2014. Progress in the
770 management of contaminated sites in Europe (JRC Reference Reports No. EUR 26376).
771 Publications Office of the European Union, Luxembourg.
772 Wyllie, M.R.J., Gregory, A.R., 1953. Formation Factors of Unconsolidated Porous Media: Influence of
773 Particle Shape and Effect of Cementation. *J. Pet. Technol. - J Pet. TECHNOL* 5, 103–110.
774 doi:10.2118/223-G
775 Yi, M.-J., Kim, J.H., Chung, S.-H., 2003. Enhancing the resolving power of least-squares inversion with
776 active constraint balancing. *Geophysics* 68, 931–941.
777 Zekkos, D.P., Bray, J.D., Kavazanjian, E., Matasovic, N., Rathje, E., Riemer, M., Stokoe, K.H., 2005.
778 Framework for the estimation of MSW unit weight profile, in: *Proceedings, Sardinia '05, 10th*
779 *International Waste Management and Landfill Symposium*, Santa Margherita Di Pula,
780 Cagliari, Italy. pp. 3–7.
781